Ultra-high-resolution dedicated brain PET with time-of-flight and depth of interaction detection (D1.7 – SGA3)

Figure 1: Living Brain assembled prototype

Assembled detector ring mounted on cart. Left: Front view, with the detector ring with the cooling system fully connected. Chiller can be seen on the bottom part. Right: Top view, with the detail on the cooling system and the electronic boards.

Project Number:	945539	Project Title:	HBP SGA3

Document Title:	Ultra-high-resolution dedicated brain PET with time-of-flight and depth of interaction detection
Document Filename:	D1.7 (D96) SGA3 M41 SUBMITTED 230926.docx
Deliverable Number:	SGA3 D1.7 (D96)
Deliverable Type:	Demonstrator
Dissemination Level:	PU = Public
Planned Delivery Date:	SGA3 M41 / 31 AUG 2023
Actual Delivery Date:	SGA3 M42 / 26 SEP 2023
Author(s):	Morera Constantino, OCV (P151)
Compiled by:	Morera Constantino, OCV (P151)
Contributor(s):	Morera Constantino, OCV (P151) and González Gabriel, OCV (P151) contributed to all Sections
WP QC Review:	Giovanna RAMOS QUEDA, AMU (P78); Lisa Otten, AMU (P78)
WP Leader / Deputy Leader Sign Off:	Viktor JIRSA, AMU (P78)
T7.4 QC Review:	Martin TELEFONT, EBRAINS (P1)
Description in GA:	Dedicated brain PET (dbPET) prototype in seating/reclined position, with time-of-flight and depth of interaction▫detection, able to produce reconstructed images with 1.0mm spatial resolution. Brain cortex thickness is 1.5-4.5mm,▫containing six layers with different functions and neuro receptors. 1.0mm 3D spatial resolution will allow to assess▫brain functional activity at cortex layer / deep nuclei level
Abstract:	This deliverable describes the development process and the obtained results of Living Brain Dedicated Brain PET. Dedicated brain PET hardware, including innovative slab-based detector crystal and exclusive electronics with signal reduction logic, has been designed, manufactured and validated. A complete housing with dedicated cooling system, portable cart and electric power system has been manufactured and integrated. Data acquisition and coincidence electronics from PETSys has been acquired, calibrated and integrated in the final solution. Software applications for data acquisition, processing, calibration and image reconstruction have been developed. The complete system includes two high performance workstations for data acquisition, processing and storage. The complete system has been calibrated, and NEMA protocol has been used for characterization of the system, showing good results. Clinical trial is approved and patients will be acquired in September.
Keywords:	Industry, brain innovation, SME, digital neuroscience, brain technologies, brain research, medicine, computing, PET, nuclear imaging
Target Users/Readers:	Clinicians, computer scientists, neuroimaging community, neuroscientific community, researchers, scientific community

Table of Contents

Table of Tables

Table of Figures

1. Introduction

The specific objective of this deliverable was to build a prototype dedicated brain PET incorporating revolutionary innovations upgrading neurophysiology knowledge, advanced neurological research, and expanding clinical applications. LIVING BRAIN Dedicated Brain PET (dB PET) has superior specifications vs whole body PET, adding also patient comfort, ergonomics and dynamic stimulus capabilities.

It is our conviction that the breakthrough development presented in this application will be adding significant value to EBRAINS, impacting positively in several major outcomes, including OC1 Enrichment of research tools, OC4 Personalized brain models, OC7 Clinical consciousness disorders and OC8 Translating EBRAINS to Medicine in multiple applications.

Adding the molecular / functional perspective to EBRAINS SC2 brain atlas will further develop / multiply its contribution to comprehensive brain knowledge. This will multiply its practical impact for both research and clinical care of healthy, altered and pathological brain, fulfilling HBP ambition and objectives.

The planned works included a limited field of view PET of 50mm field of View. Using external funding in collaboration with the i3m institute, the final assembled system is a fully functional brain PET with 200mm axial field of view. The prototype has been manufactured and is currently being assessed, with the first patients expected on September.

2. System Hardware

The dedicated brain PET prototype is composed of the following components:

- Detection ring, composed of 8 rings of detector modules and its accompanying electronics.
- System housing, which is a portable cart enclosing the detection ring, the electronics subsystem and the cooling subsystem.
- Reconstruction and data processing station, composed of two dedicated workstations.

Each of the components is described in detail in the following sections.

2.1 Detector modules

The core components of a Positron Emission Tomography (PET) system are the detector modules. A detector module is composed of a scintillator crystal, that interacts with the emitted high energy photons and produces light; and a photomultiplier coupled to the crystal, that converts the light to an electric signal. This signal is conditioned and processed with dedicated electronics to extract the information that will be used to produce an image.

The Living Brain system is composed of 8 rings, each of which has 40 detector modules.

2.1.1 Crystal design

Living Brain detectors are based on the use of inorganic LYSO (Lutetium Yttrium Oxyorthosilicate) scintillator crystals with a semi-monolithic geometry (slabs): one of the axes is pixelated, with 1.52mm pixel size, while the other axis is continuous. LYSO material is one of the most widely used scintillators in PET technology. BGO (Bismuth Germanium) based scintillators are also widely used because of their low cost, but they have a very slow decay constant, which makes them unsuitable for time-of-flight measurements and they generate 4 times less photons per MeV than LYSO crystals. Semi-monolithic crystals (slabs) offer the possibility of combining spatial resolution, photon interaction depth and high temporal performance.

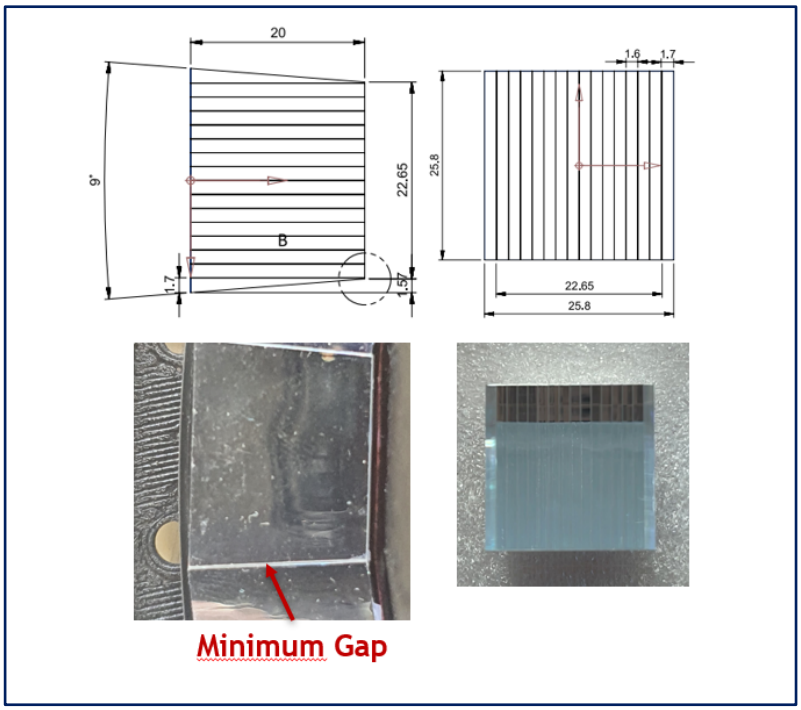

Figure 2: Design of the scintillator crystal

Top: Plans and dimensions of scintillator crystal block. Bottom: Actual crystal block manufactured.

The size of each slab on Living Brain is 25.8mmx1.52mmx20mm (width x height x thickness), resulting in a crystal block of 25.8x25.8x20mm (width x height x depth). The lateral slabs are trapezoidal to minimize the dead areas of the ring (see Figure 2).

The complete system is composed of 8 rings, each of which has 40 detector blocks, totalling 320 detector blocks (5.120 slabs)

2.1.2 Detector electronics

Each crystal block is optically coupled to a 8x8 array of solid state Silicon MPPC (Multi-Pixel Photon Counter) S13361-3075 Photomultipliers (SiPM), manufactured by Hamamatsu, with the following technical specifications:

- $1.7x10^6$ gain
- 64 channels (8x8)
- 3x3mm photosensive area/channel
- Pixel pitch: 75 µm
- 74% fill factor
- 40% photon detector efficiency
- 450 nm peak sensitivity wavelength
- 1.55 refractive index

Each Silicon photomultiplier is connected to a readout electronics board with channel reduction logic. This electronic board reduces the number of output channels from 64 (8x8) to 16 (8+8), using a patented Rows and Columns logic (see Figure 3). For the complete PET system, the total number of channels is reduced from 20.480 to 5.120 channels, reducing the costs and the required bandwidth.

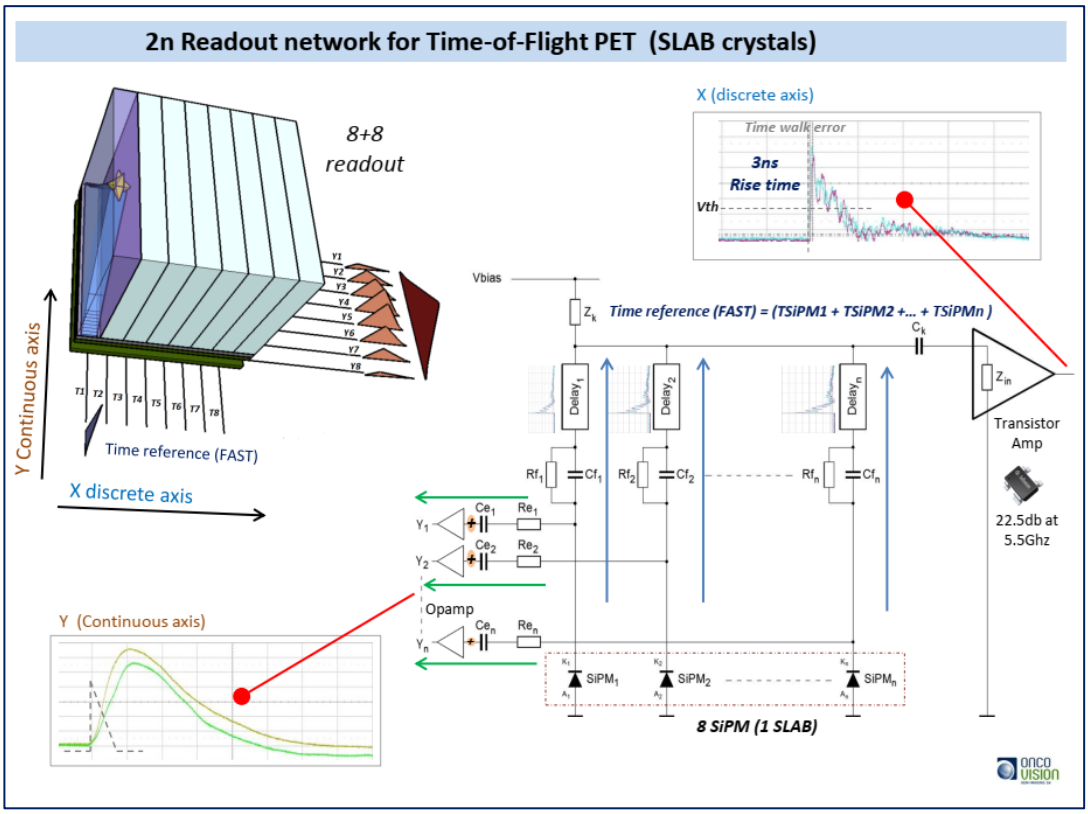

Figure 3: Readout network

Additional electronic board for signal amplification and distribution have been also designed and manufactured. Each amplifier board feeds 2 detector blocks, and each distribution board feeds 4 amplifier boards (8 detector blocks). The electronics for the complete ring of detector contains 320 SiPM arrays, 320 readout boards, 160 amplifier boards and 40 distribution boards (see Figure 4).

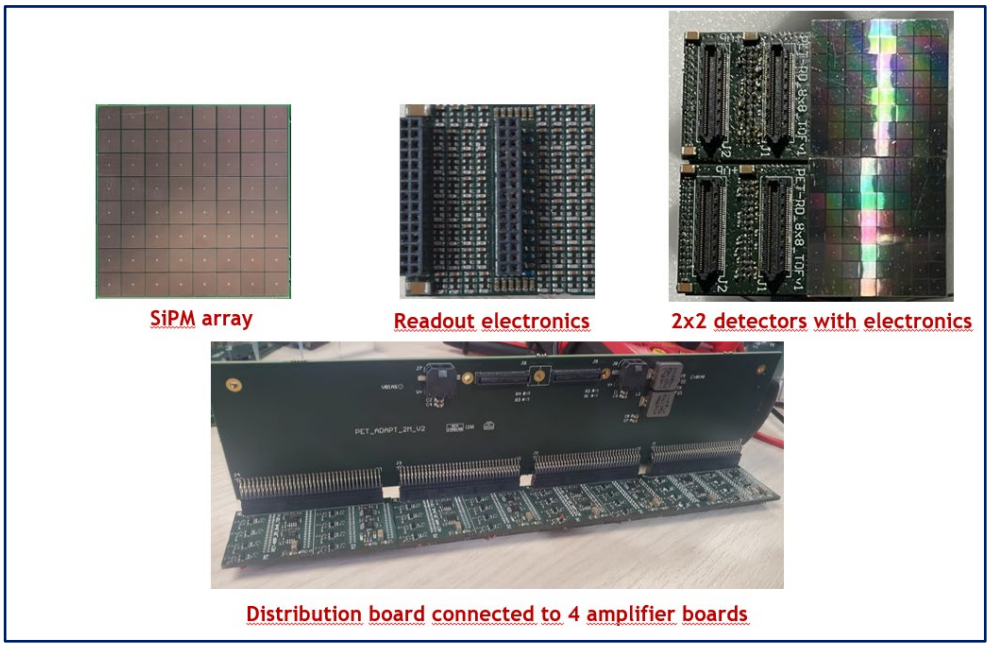

Figure 4: Detector electronics

2.2 Electronic subsystem

The complete electronic subsystem has the following elements:

- Detector electronics. This element has already been described and comprises the Silicon photomultiplier array, the readout electronics and the amplifier electronics.
- Acquisition and clock electronics. The acquisition electronics comprises specialized electronics by PETSys, Inc. Data capture electronics includes a dedicated ASIC and Clock/Coincidence electronics, plus a data acquisition PC card.
- Power electronics and electric panel.

2.2.1 Acquisition electronics

The solution chosen for data acquisition is a commercial solution from the Portuguese company PETsys. It is a highly scalable hierarchical (or multilevel) solution where the addition of electronic modules allows increasing the number of channels.

On the other hand, the cost is proportional to the number of channels, as well as the bandwidth and volume of data generated, which is why the channel reduction logic already mentioned in the readout card has been incorporated. Living Brain has a total of 320 modules with 8x8 SiPMs each, equivalent to 20,480 sensors, which with signal reduction is 5,120 channels.

The complete read chain (Figure 5) consists of the following functional blocks:

- **ASIC TOFPET2**, capable of reading 64 channels. When a channel exceeds a programmable threshold, the ASIC stores a time stamp, the measured electrical charge and the channel number. This digital information constitutes a 'hit' or event. The ASICs are mounted on a readout board (called **FEM256**), which contains 4 ASICs and is capable of reading 256 channels (equivalent to 16 detector blocks). The ASIC requires a cooling system to limit the temperature of the ASICs and keep them around 20-25 ºC. Living Brain uses 20 FEM256 boards for the 320 detector.

- 1024-channel concentrator board (called **FEBD/1k**). It concentrates the various incoming data streams on a high-speed optical or copper link (SFP+) that is sent to the acquisition module on the PC. It also provides control and synchronization to the first-level modules. Living Brain uses 5 FEBD/1K for connecting the 20 FEM256 boards.
- Trigger and Synchronization board (**CLK/Trigger**). Provides synchronization and triggering to up to 16 FEB/D (therefore only one is used for Living Brain). Connects to the acquisition module on the PC. A trigger signal is generated when matching events are detected within a time window of programmable size.
- Data acquisition board (**DAQ**). With three SFP+ connectors, it connects to a trigger module and up to three chains of concentrator modules. Allows a maximum of 200 Mcps (millions of coincidence events per second). It sorts events by timestamp for easy processing on the PC. Living Brain has two FEBD/1k connected on the first two connectors and on the third one it has a FEBD/1k and the trigger module.

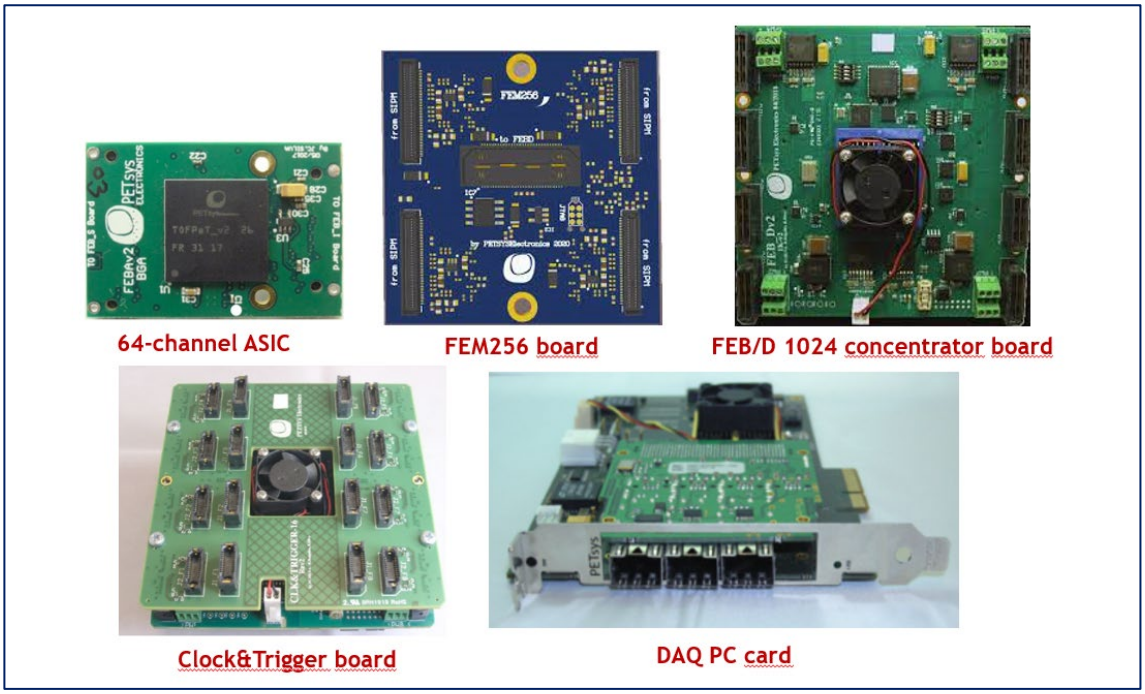

Figure 5: PETSys read chain

2.2.2 Power electronics and electric panel

In the initial design of the PCB, 3V low noise power supplies were selected, which had very specific requirements in terms of voltage and intensity. Due to the high lead times, PCB have been redesigned to use standard 24V power supplies and DC/DC adapters, with specific filtering to reduce ripple. The boards that contains the DC/DC converter and filters have been designed in-house, while the 24V power supply are standard TDK-lambda modules.

Living Brain input power is isolated with a Toroid Talema Isolation Transformer, which protects electronics and also operator and patients from any peaks in the power supply. The power button is connected to a safety rele with a timer. There are three AC/DC converters: two 24V (one for the chiller and one for the DC/DC adapters) and one 12V for the PETSys digital boards (Figure 6).

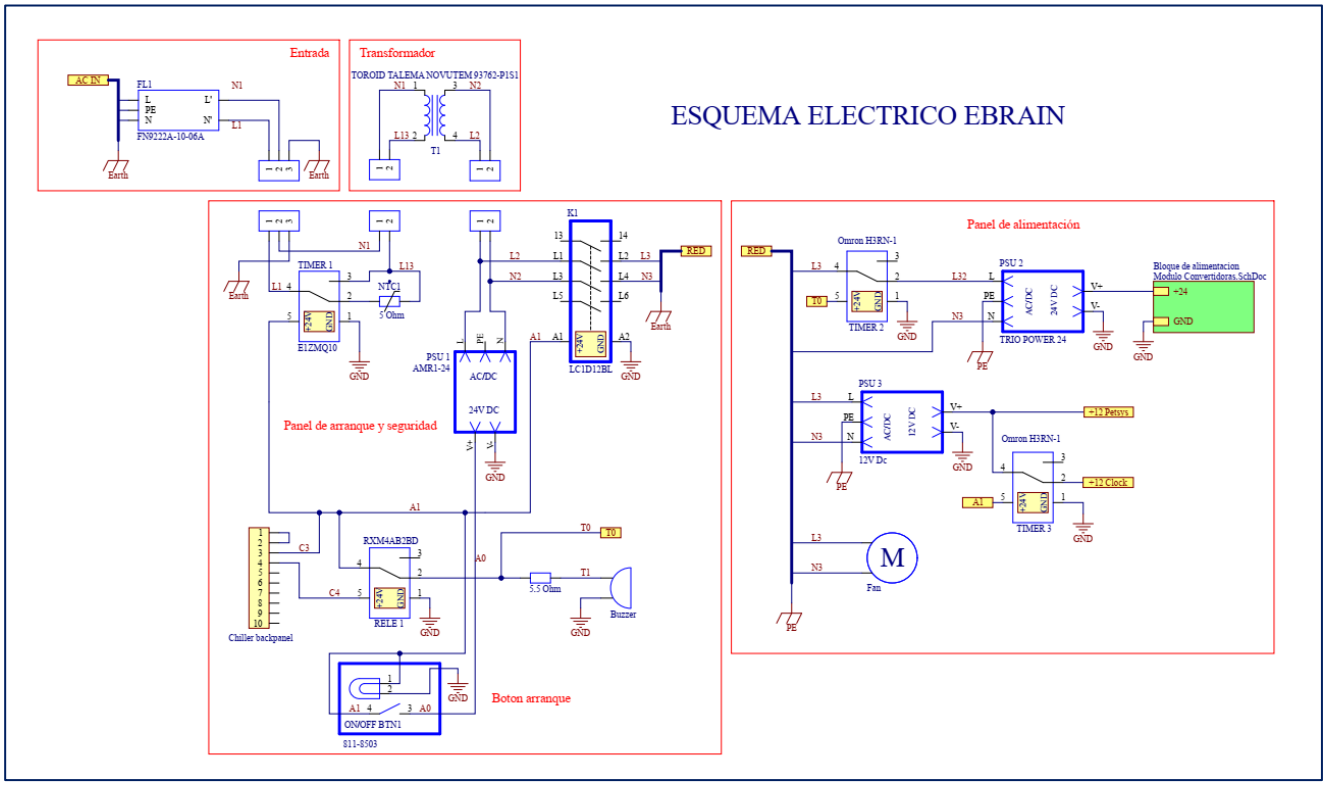

Figure 6: Living Brain electrical schematic

2.3 Housing and mechanical components

The complete system includes the detection ring, a mobile cart with all the subsystems embedded and the cooling system.

2.3.1 Mechanical design

The living brain ring is attached to a mobile cart with two fixed wheels and two rotating wheels. The wheels have a brake to fix the cart during acquisition (Figure 7). The ring's axial axis has been placed horizontally, which allows the Living Brain system to acquire with the patient lying on a standard stretcher. A custom headrest has been designed for attaching to the stretcher. The ring has two heavy load hinges for placing it horizontally, for maintenance purposes.

The cart has been adapted from the successful and clinically validated Mammi PET cart from Oncovision (Figure 8).

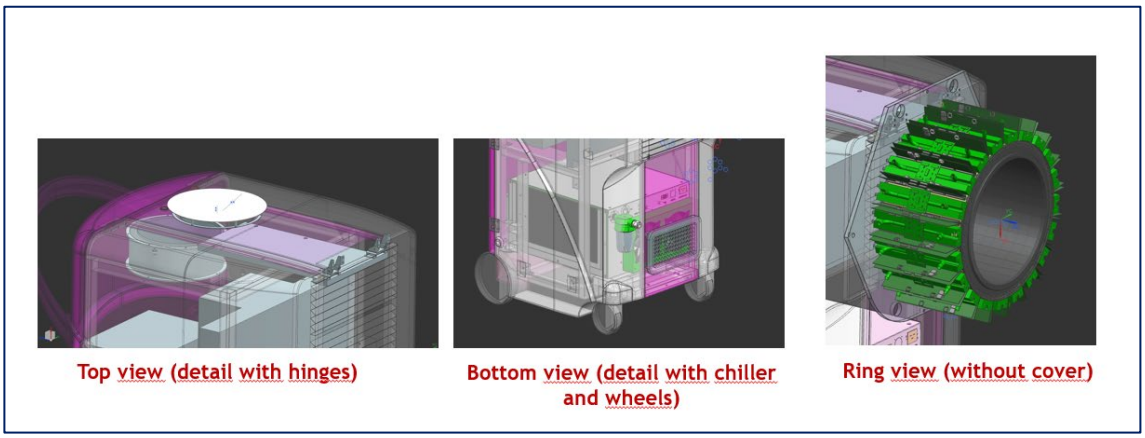

Figure 7: Living Brain cart design and mechanical details

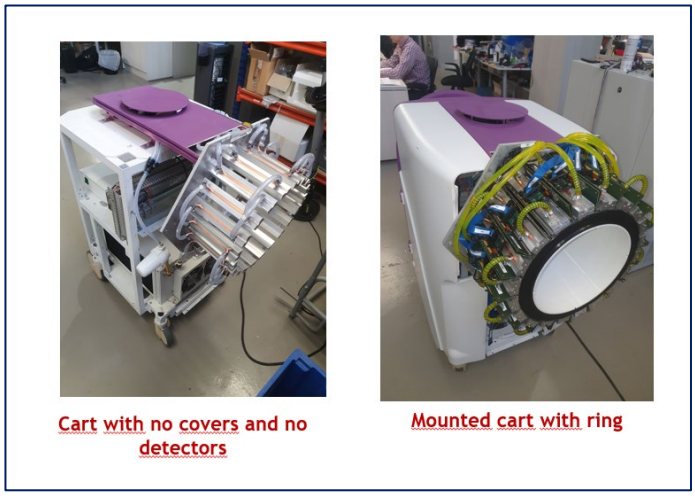

Figure 8: Assembled cart pictures

2.3.2 Cooling system

PETSys ASIC requires very stable and controlled temperatures to guarantee the accuracy of the readings that allow reliable time of flight measurements. Once the ASICs are calibrated, the temperature of the ASICs must be kept around 20-25 ºC and must be very stable.

Several cooling options were considered for Living Brain, including forced air, Peltier cells and water-cooling system. The selected cooling system has been the system recommended by PETSys, which is composed of the following elements (Figure 9):

- Water-based recirculating chiller that feeds a closed circuit of water tubes.
- Aluminium cold plates that are directly in contact with the ASICs and the water circuit.
- Thermal pads for homogeneous distribution of temperature in the electronics

Chiller is configured to work with a water temperature of 18º, which guarantees the ASICS to be between 20 and 22º.

In addition to the cooling system, Living Brain must be installed in a room with controlled temperature (< 24º) and humidity (<50%) to avoid water condensation.

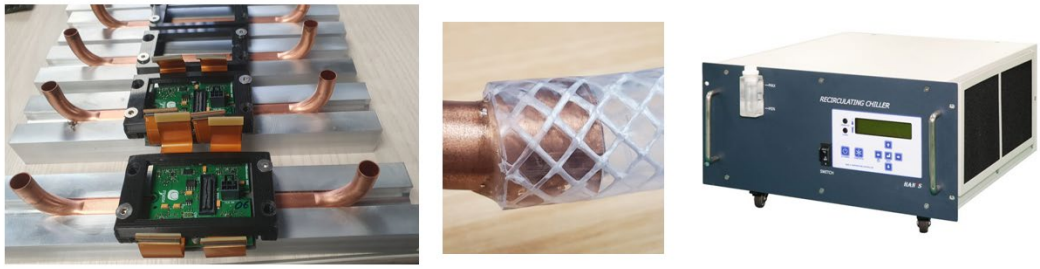

Figure 9: Cooling system components

2.3.3 Detection ring

The detection ring encloses all the detector modules, the detection and amplifier electronics, the cold plates and the cooling system. To ensure the coverage of almost all the areas of the human brain, the 4D-PET employs 320 detector elements forming a cylinder with an axial length of 200 mm and an internal diameter of 280 mm. As seen before, each detector element is composed of an array of 1×16 slab-shaped LYSO elements optically coupled to an 8x8 array, which generate 8+8 output signals through a specific readout board with signal reduction logic. These 8+8 output signals are connected to the TOFPET2 ASIC from PETsys.

Since each ASIC board works with 256 signals, the detectors have been grouped in "Super-Modules" of 16 detectors (256 signals), forming two rows of 8 detectors (one row covers the full axial field of view – 200 mm-). See Figure 10 and Figure 11.

The full ring is then formed of 20 Super-Modules.

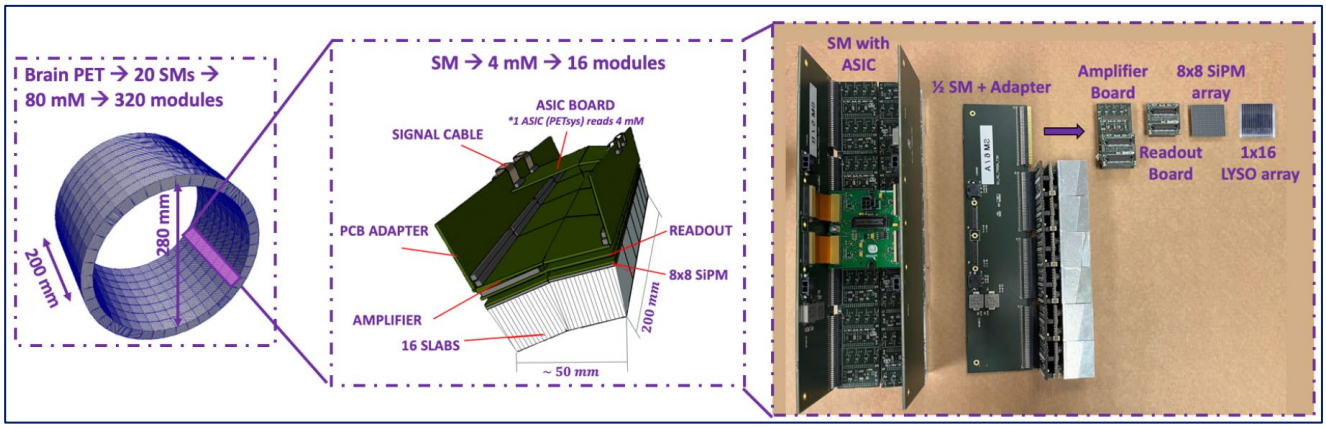

Figure 10: Ring electronic components

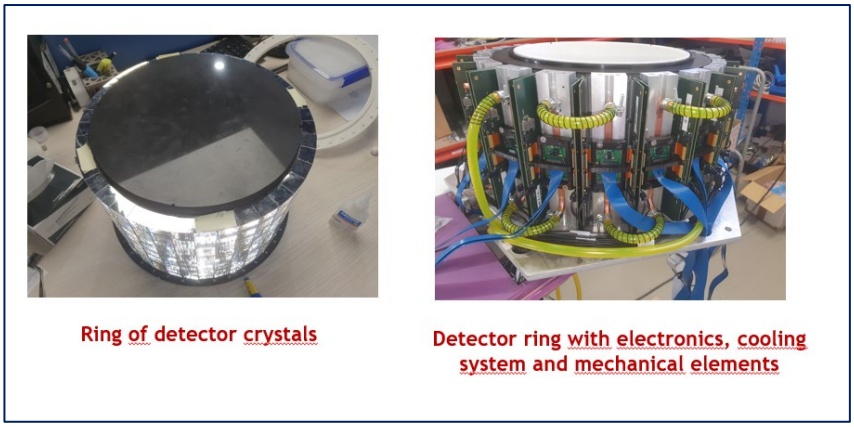

Figure 11: Mechanical ring components

2.4 Workstations

Living Brain uses two separate computers: one for data acquisition and processing, and a separate one for data calibration, GPU reconstruction and data storage (Figure 12). The computer specifications are the following:

Acquisition Workstation:

- 2 x AMD 7282 2.8 GHz processors (turbo enhanced up to 3.2 GHz), 16 cores (32 processes), 64 MB Total cache, Maximum consumption 120 W
- MZ92-FS0 Dual Board, 32 memory banks, VGA 2D Video Graphic Adapter 1920 x 1200, integrates 2 PCI-E 4.0 portsx16, 1 PCI-E 4.0 x 16 mezzanine, 2 x 1000 Network (gigabyte) cards Intel i350. IPMI 3.3 with full remote management of KVM over LAN and own mouth

- 128GB DDR4/3200 MHz ECC memory on 16 x 8GB modules
- 1 NVidia RTX 3090 blower GPU card, 24 GB GDDR6X RAM with one bandwidth 19.5 Gbps, 10,496 CUDA cores per card, maximum power consumption 350 W. Technology Ampere. PCI-E 4.0 BUS requires CUDA 11
- Dual 10GBASE-T Intel X550 Card
- 1 x 3.84TB Kioxia NVME 2.5" U3 drive, with a read speed of 1,000K IOPS and 60K IOPS write, for Scratch
- 1 x 960GB 2.5" PNY SATA CS900 SSD with 89,000 read performance 87,000 IOPS and write IOPS, 6Gb/s, for OS
- CentOS 7 Operating System (required by PETSys DAQ card)

Reconstruction Workstation:

- 2 x AMD 7282 2.8 GHz processors (turbo enhanced up to 3.2 GHz), 16 cores (32 processes), 64 MB Total cache, Maximum consumption 120 W
- MZ92-FS0 Dual Boar, 32 memory banks, VGA 2D Video Graphic Adapter 1920 x 1200, integrates 2 PCI-E 4.0 portsx16, 1 PCI-E 4.0 x 16 mezzanine, 2 x 1000 Network (gigabyte) cards Intel i350. IPMI 3.3 with full remote management of KVM over LAN and own mouth
- 128GB DDR4/3200 MHz ECC memory on 16 x 8GB modules
- 2 NVidia RTX 3090 blower GPU card, 24 GB GDDR6X RAM with one bandwidth 19.5 Gbps, 10,496 CUDA cores per card, maximum power consumption 350 W. Technology Ampere. PCI-E 4.0 BUS requires CUDA 11
- Dual 10GBASE-T Intel X550 Card
- LSI 3108 Raid controller with 12 GB / s and 1 GB cache 8 ports. Raid 0, 1, 5, 6, 10, 50, 60
- 8 x Samsung MZ-77Q8T0 8TB SSDs, 2.5" 6Gb/s, read capable 98,000 IOPS and 88,000 write IOPS. 56 TB Net in RAID 5, for data storage
- Windows 11 Professional Operating system (required by GPU reconstruction software)

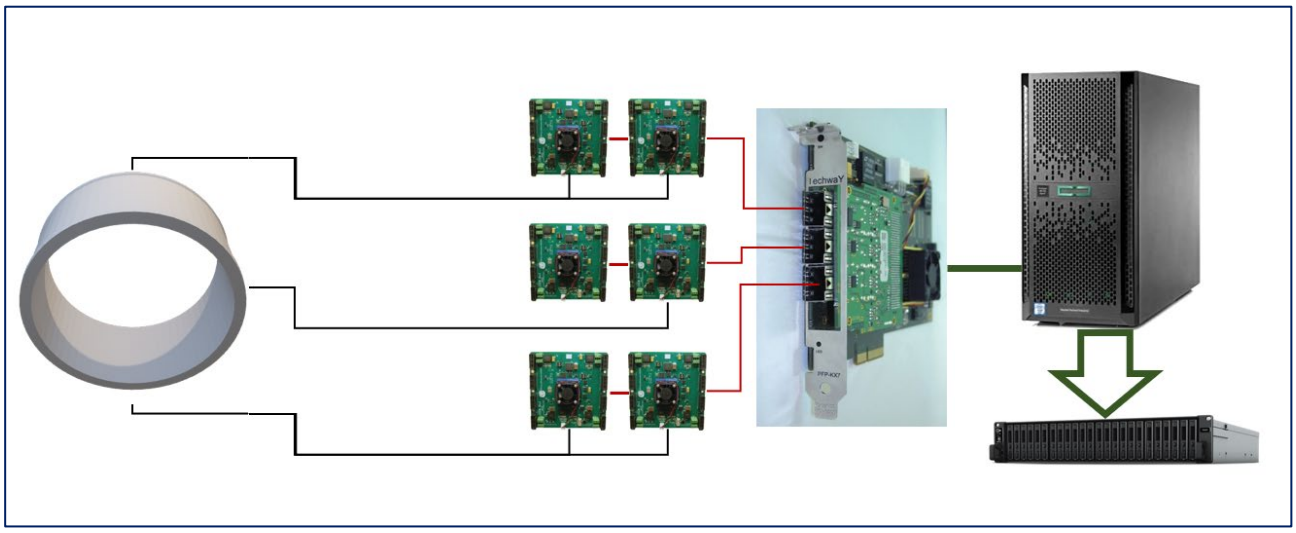

Figure 12: Workstations and data connections

Acquisition workstation is connected to the Living Brain system through a PETSys DAQ card (installed on PCIx16 slot). Reconstruction workstation is connected to the acquisition workstation with a 10-Gbit direct connection, forming an intranet without external connections.

3. Data processing, calibration and reconstruction

In order to generate an image, data acquired from the system needs to be processed, calibrated and reconstructed. The complete process includes many different steps (Figure 13), each of which has specific algorithms.

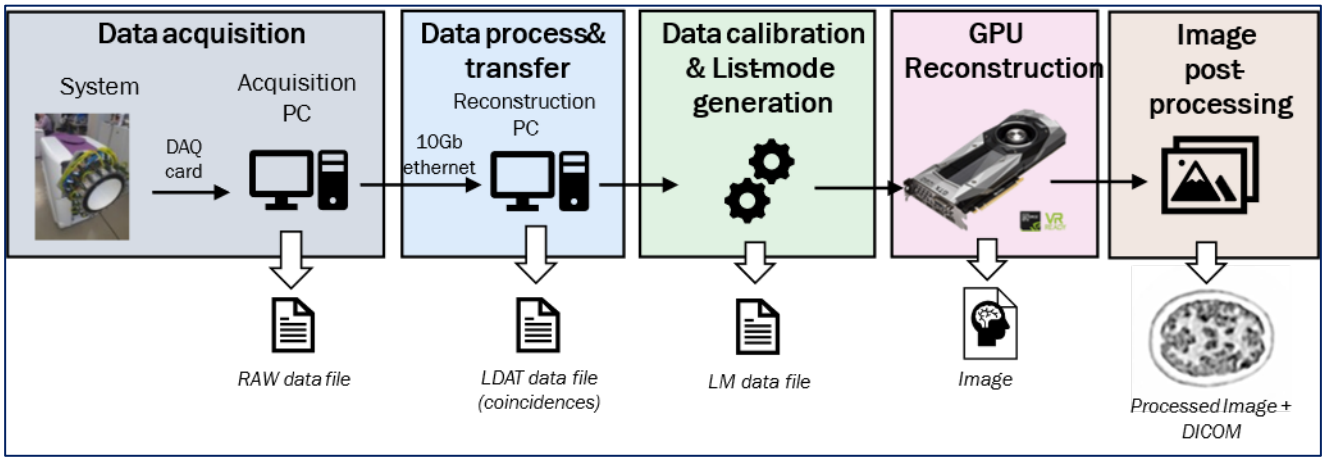

Figure 13: Processing and reconstructiron steps.

3.1 Acquisition software

The software used for data acquisition, as well as data processing (which includes coincidence search) is the software provided by PETSys for controlling the PETSys hardware and communication cards.

Before being able to acquire, the ASICs must be auto-calibrated. This is an internal process for adjusting thresholds and other electric parameters that allow to properly measure times and electric charge of all analog channels. This calibration needs to be done only once, unless electronic elements or environment conditions (such as temperature, which is why a cooling system is needed) are changed.

In addition to the ASIC calibration, the electrical channel IDs need to be mapped to the physical super-modules and its position in the ring. Also, the valid coincidences need to be also defined and configured.

Once the ASICs are calibrated and the system is properly configured, PETSys is ready for acquiring data using the provided software tools.

3.1.1 Data acquisition

The software that PETSys provides for data acquisition includes a GUI application that allows to setup the acquisition parameters (Figure 14).

The data can be acquired and processed in a single step or in separate steps. If more than one acquisition is planned, it is recommended to do a separate step for data processing. Otherwise, the second acquisition won't start until data processing is finished.

Data acquisition options are:

- Mode: Must be 'QDC' for reading the signal charge
- Time: Must be specified in seconds.
- HW Trigger: Must be set to 'On'

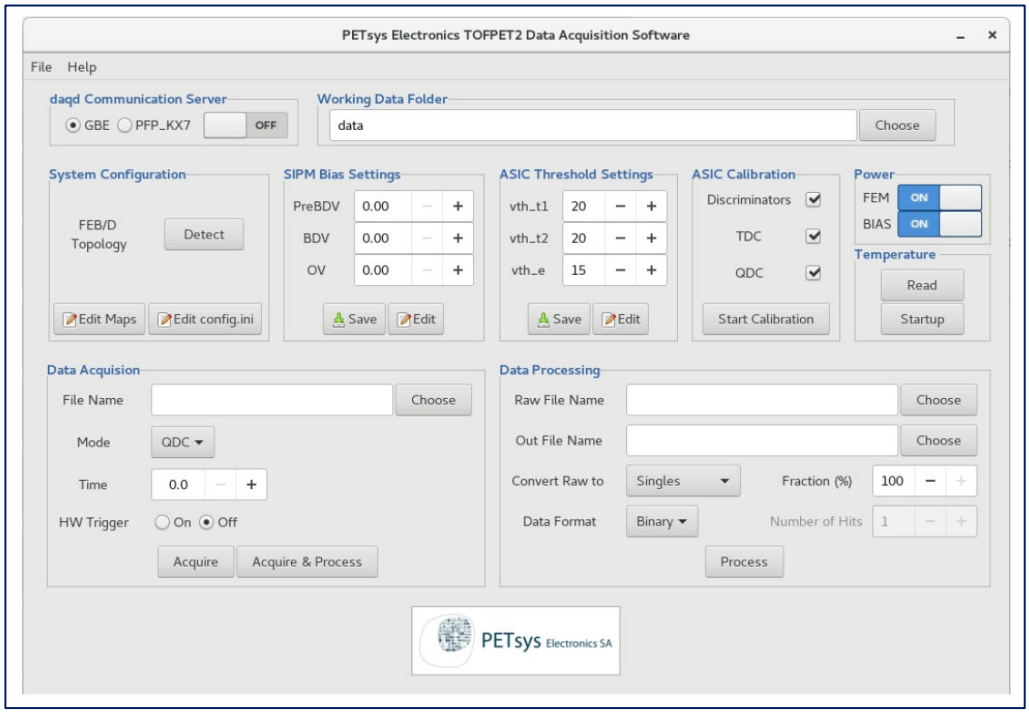

Figure 14: PETSys data acquisition software

Software will acquire a '.rawf' binary file containing all captured events. These events must be processed to obtain the coincidences, adjusted with the pre-calibrated ASIC parameters.

3.1.2 Data processing

Data processing is done with the same application, and processing options are:

- Raw File Name: Enter or select the '.rawf' file to process
- Out File Name: Leave default value.
- Convert Raw to: Must be set to "Coincidences"
- Fraction: Must be set to 100%
- Data Format: Must be set to "Binary"
- Number of hits: Must be set to 64. This is the maximum number of channels that can be triggered in a single coincidence, which will depend on the hardware. For Living Brain, standard number of channels should be 11 on each module (8 of the monolithic slab axis and up to 3 neighbour slabs). Leaving 64 allows detecting double and triple coincidences.

Processed coincidence data is written in a binary '.ldat' file, that contains a sorted list od coincidences, each of which contains all the active channels and their measured times and charges. This processed data still needs to be calibrated to obtain the actual impact position, energy, depth of interaction and time of flight.

3.2 Calibration steps

The processed data needs to be calibrated. The different calibration steps are positions calibration, energy calibration, Depth of interaction calibration, time of flight calibration, uniformity calibration and normalization.

The developed algorithms and calibration processes for Living Brain are described in detail in the following paragraphs.

3.2.1 Position calibration

The position calibration allows to obtain the actual impact position of a photon in the crystal. It consists of two coordinates: X (along the pixelated axis) and Y (along the monolithic axis).

X coordinate can be directly extracted by obtaining the SiPM X channel with the maximum energy, which corresponds to the physical slab that receives the impact and generates the light. Living Brain has two slabs per SiPM channel, so a logic comparing neighbour SiPM channels was added, making sure all slabs have equal number of hits when a uniform source is applied.

For obtaining the Y coordinate, a neural network (NN) model was implemented consisting of a multilayer perceptron architecture, with an initial embedding layer that codifies slab information (Figure 15). For training the network, coincidence data was acquired by displacing in 1mm steps a slit collimator (250µm) with a 22Na source between two SM. For data acquisition along the monolithic direction, the slit was placed perpendicular to the slabs.

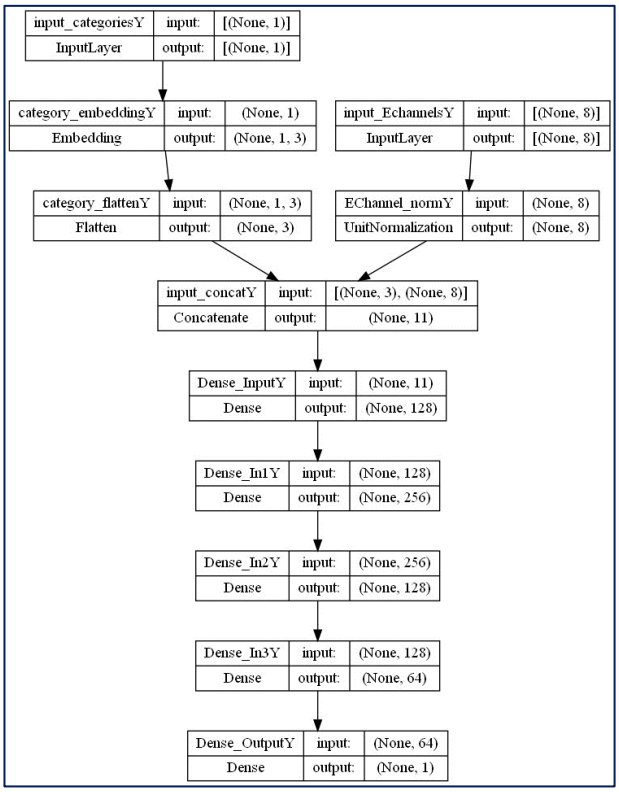

Figure 15: Neural network topology

The activation function used was the RELU, and the loss function was the Log-Cosh function, with the Nadam optimizer for gradient descent. Fig. 3 shows the FWHM (Full-width half maximum), MAE (Mean average Error), and bias obtained after training the NN. The NN prediction yielded average FWHM of 2.1±1.0 mm, and MAE of 1.1 +- 0.5mm (Figure 16).

Calibrating individually all 5.120 slabs requires many acquisition and training time, so only one Super-Module (256 slabs) is fully calibrated. The assembly process guarantees similar behaviour between slabs with small variability. The uncalibrated slabs are mapped to the calibrated ones by measuring the light distribution with a uniform source. This creates ‘categories’ of similar slabs, which are encoded on the Neural Network and are part of the final calibration.

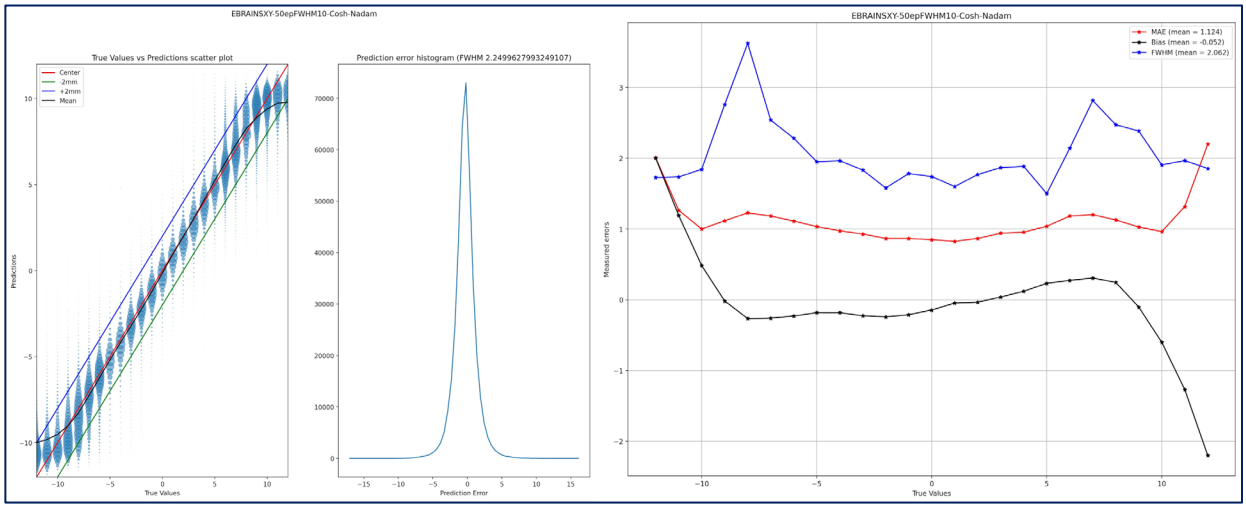

Figure 16: NN training results (Y position, full Super-Module)

3.2.2 Energy calibration

Energy calibration converts measured charges on each channel to physical keV units. To do so, a channel equalization is performed to guarantee the photopeak is at the same position. Then, all the slabs also need to be equalized to compensate the different gains for each slab (Figure 17). Finally, accumulated peak is dynamically monitored to correct any deviations because to temperature or rate changes.

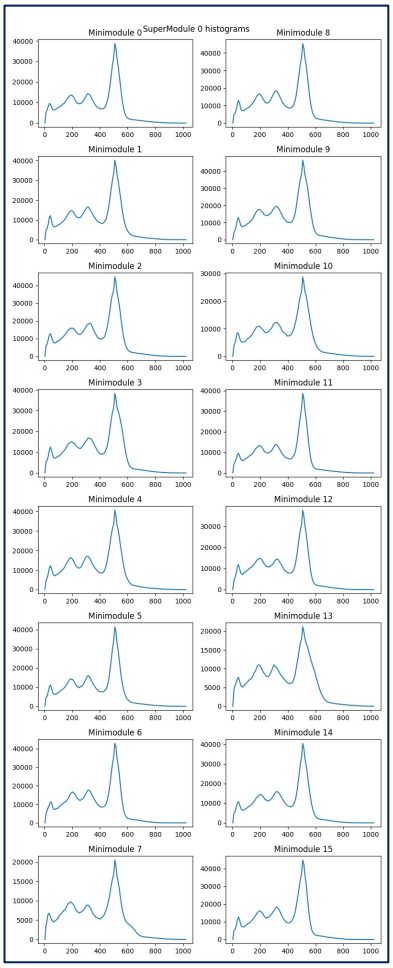

Figure 17: Equalized energy peaks

3.2.3 Depth of interaction calibration

The depth of interaction (DOI) is the distance that a photon covers from the time it penetrates into the detector crystal until it deposits all its energy, producing scintillation. PET detectors that do not estimate the DOI usually use a fixed value to the DOI which can be localized on the surface of the crystal or from estimation of the mean DOI. The error in the estimation of the real position of the impact produces an error in the line of response known as the parallax error. The greater the distance from the field of view (FOV) the greater the error. The parallax error can produce significant deviations of the real position, translating into blurring in the reconstructed image and less clinical resolution according to the distance from the centre of the FOV.

The DOI calibration allows to obtain the actual depth of the impact of a photon in the crystal (Z coordinate), which enables parallax error correction.

For obtaining the Z coordinate, another neural network (NN) with the same topology as the network for Y coordinate was implemented. The network was trained with the same slit, but placed laterally to the slabs. The NN prediction yielded average FWHM of 3.4 mm (Figure 18).

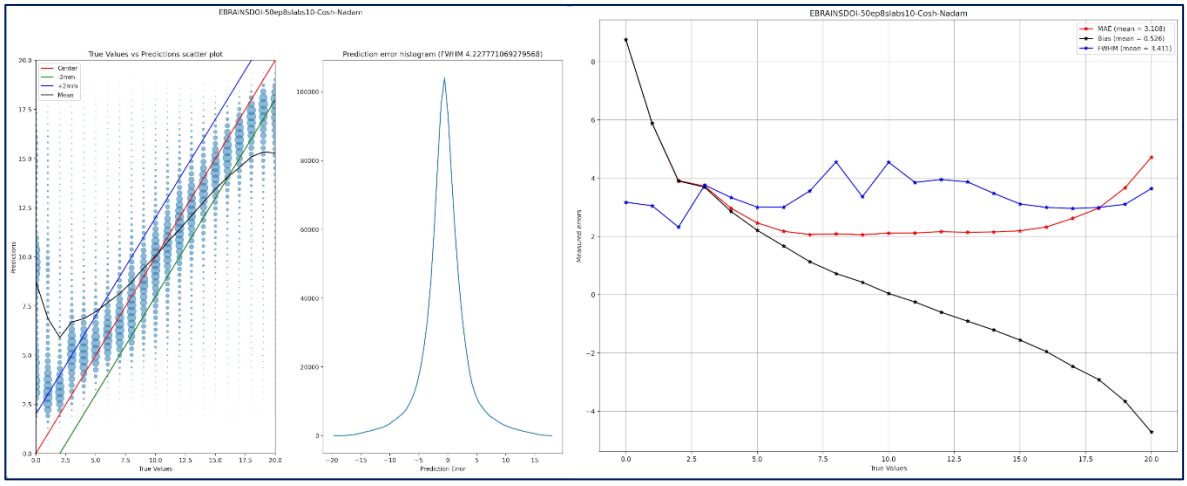

Figure 18: NN training results (DOI, full Super-Module)

Both Neural Networks (Y and DOI) are them combined in a single model for obtaining the two coordinated in a single network

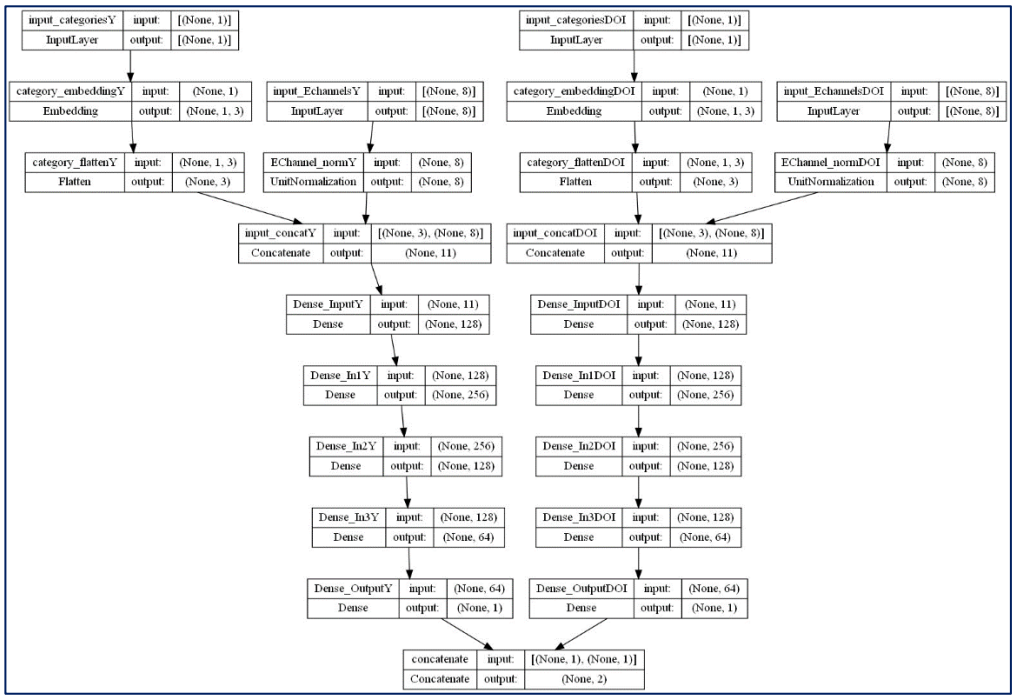

Figure 19: Combined Neural network topology

As for the Y network, only one Super-Module is calibrated and the uncalibrated slabs are mapped to the calibrated ones by measuring the light distribution with a uniform source.

3.2.4 Time of flight calibration

Time of flight is directly measured as the difference between the timestamps of the two events of the coincidence. Only the events on the pixelated axis (slab events) are considered. Time of flight measurement reduces the uncertainty of the actual disintegration position along the line of response, which improves the signal to noise ratio and the reconstructed image quality. Images with time of flight require much less statistics than images without time of flight for producing similar results.

But first, the time offsets on each channel need to be compensated. This is known as the time skew correction. Time skew is produced by the different paths of the signals, as well as other effects producing a delay on the trigger, such as signal rise time. To compensate these offsets, a source is placed in a known position (with a known time-of flight), the time-of flight of the detector blocks close to the source is measured and compensated. For Living Brain, linear sources are placed on a quadrant, close to the modules (Figure 20).

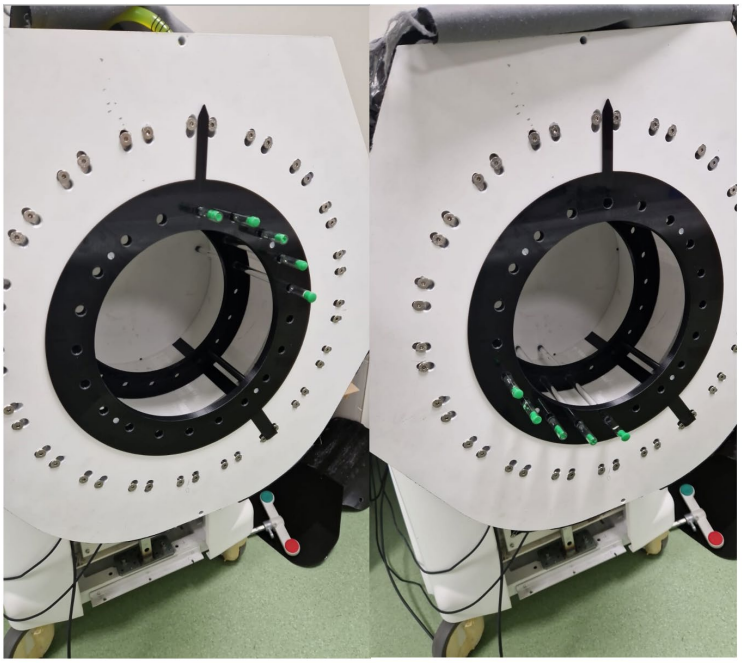

Figure 20: Skew calibration at different quadrants

3.2.5 Uniformity calibration

Uniformity calibration corrects detector crystal efficiency at detector surface. PET reconstructed images are not uniform, due to two different factors: detector efficiency and geometric efficiency. The most relevant factor for monolithic and semi-monolithic crystals is detector efficiency, because the border effects produce many artifacts. Event though the normalization can correct this problem, the statistics needed is very high (there are many different LORs). On the other hand, the statistics for correcting the effect directly on the crystal surface (correcting per pixel instead of per LOR) is two orders of magnitude lower, generating cleaner images.

To calibrate the uniformity, a centered uniform source is acquired for a few minutes. The impact map on all detectors is measured and corrected (Figure 21).

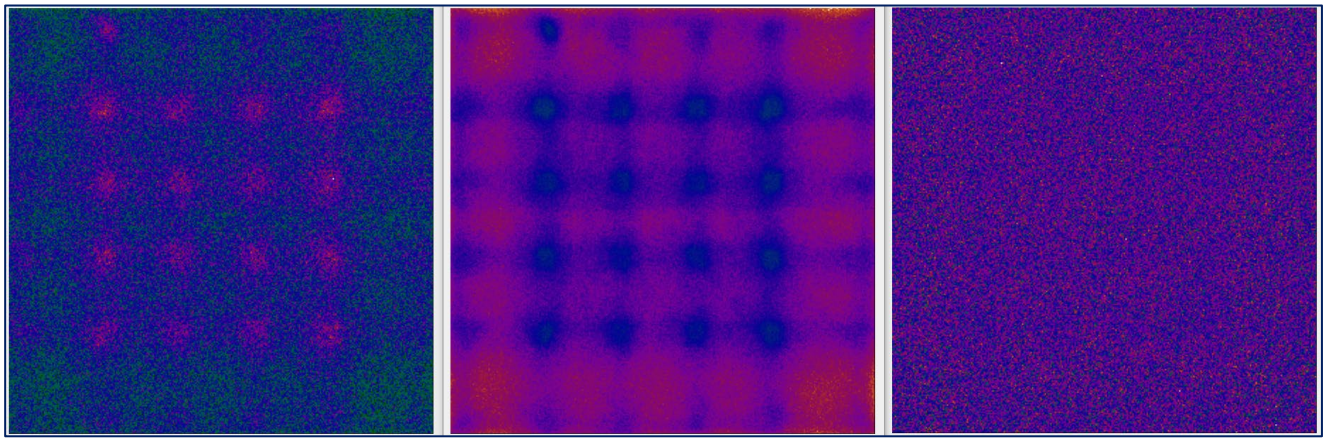

Figure 21: Uniformity calibration

3.2.6 Normalization calibration

The normalization calibration uses a phantom with uniform distribution of activity across all LORs to correct any inhomogeneity of the system. As commented, this inhomogeneities can be originated on the detector (crystal, optical coupling or electronic gain), on the system geometry, or due to the different coincidence detection efficiencies. The detector effects are corrected with the uniformity calibration.

For correcting the other effects, the theorical distribution of the activity on each LOR is compared with the measured distribution of activity, and a correction factor is calculated for each line of response. The data needed for this calibration is very high, since the number of lines of response can be very high. For Living Brain, the number of lines of response is 1.761.607.680, and at least 100 times more data is needed for correction.

The phantom used for calibration is a uniform ring with a narrow line of active area (Figure 22).

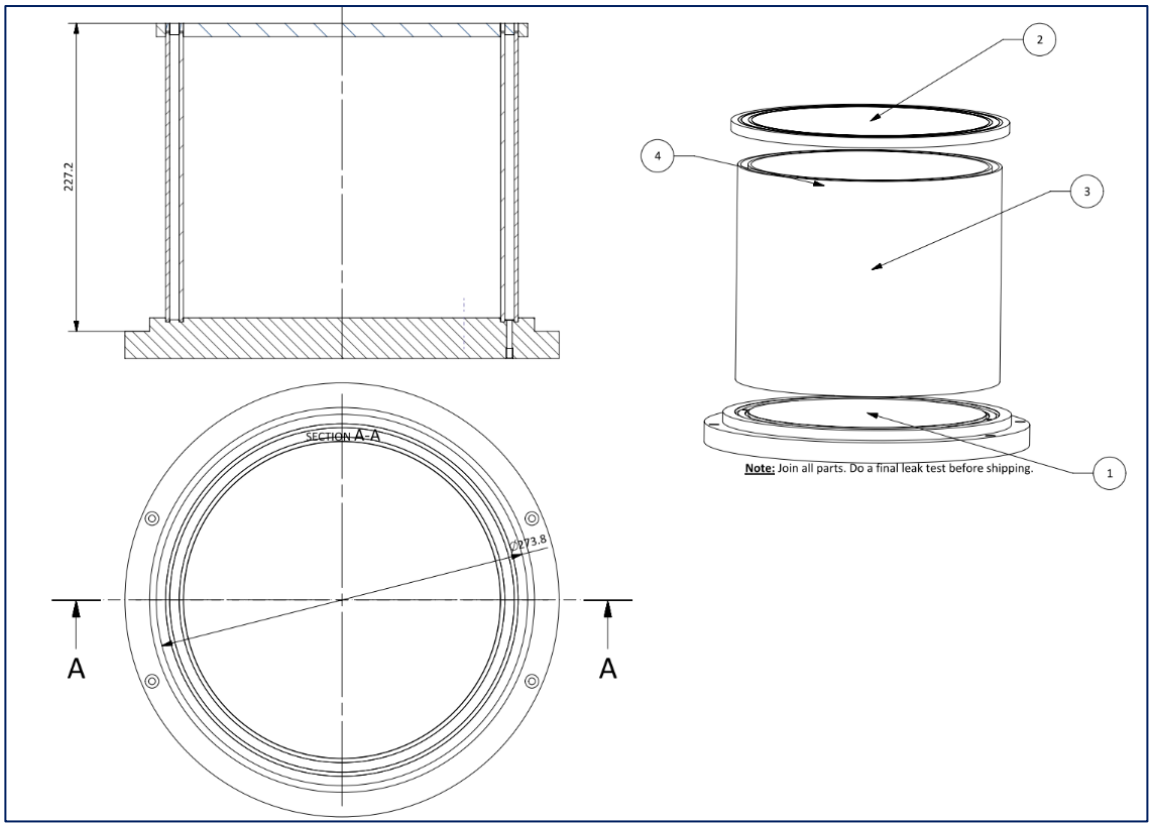

Figure 22: Normalization phantom dimensions

3.3 Image reconstruction

A dedicated software for image reconstruction has been developed (Figure 23). The software allows selecting reconstruction algorithm (MLEM or OSEM), projector (Solid Angle or Orthogonal distance), number of iterations and subsets and some other options such as the active corrections (Scatter, Randoms, Attenuation).

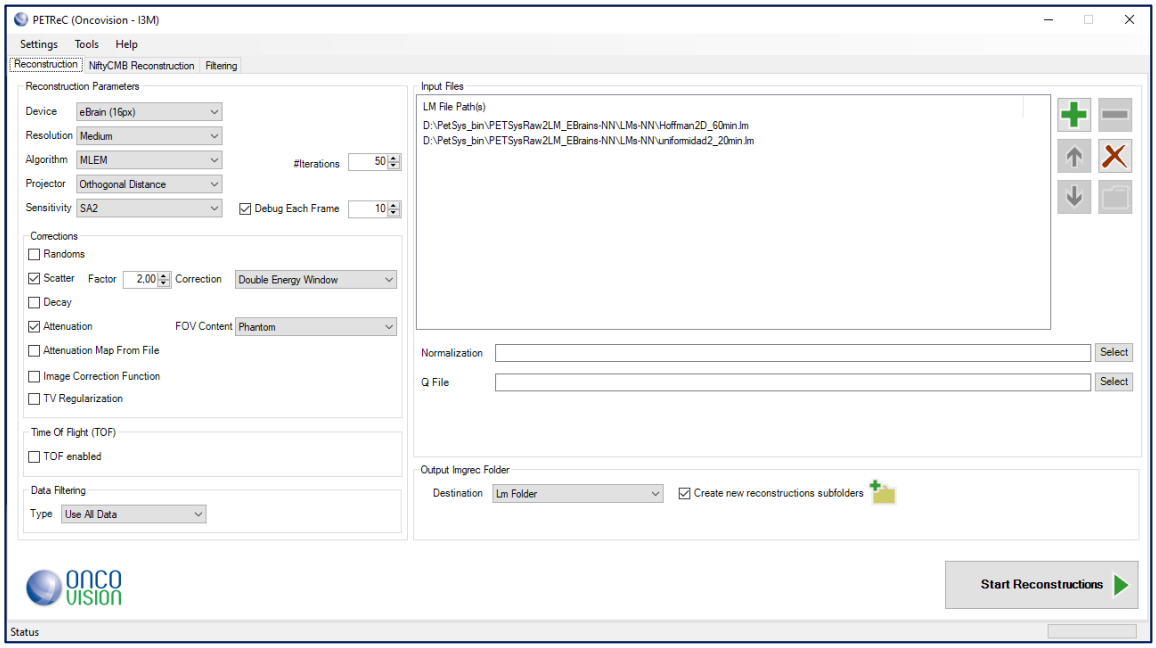

Figure 23: Reconstruction software interface

3.3.1 Reconstruction algorithm

Images are reconstructed employing in-house developed code. No external imaging software was used. Reconstructed images use an OSEM algorithm with 12 subsets and 4 iterations, or an MLEM algorithm with 50 iterations. The reconstructed field of view contains 322 x 322 x 256 cubical voxels of size 0.8 x 0.8 x 0.8 mm3. A regularization step based on the minimization of the total variation functional is performed between subiterations. The final images are postfiltered using a standard median filter with kernel size 3.

Time-of-flight reconstruction is performed using temporal bins. The time of flight is encoded as a weight of each event in a temporal bin. This generates multiple histograms with overlapped temporal bins that are reconstructed individually, and the reconstructed images combined to generate a single image.

3.3.2 Corrections

Scatter or photon dispersion in PET occurs when one of the photons collides with a free electron and deviates, losing part of its energy. The system detects an incorrect coincidence since the photon has deviated. The scatter events in a brain PET image typically represent 30% of all the coincidences detected. The scatter effect in the image is observed as a loss of spatial resolution, noisy images and the transfer of counts from the most active to less active zones. This effect also alters the uniformity of the image and affects correct quantification and also depends on the density of the material passed through, being much more probable when passing through dense materials such as the cranium. Scatter correction in Living Brain is performed a dual energy window. Events in the low energy window are used to estimate the scattered events, and scaled to correct on the trues energy window.

Attenuation in PET is the loss of detection of events of coincidence due to their absorption in human tissues. The greater the path the photons follow, or the greater the density of the tissues through which they pass, the higher the percentage of photons absorbed. This produces an unequal distribution of activity in the images obtained, showing the external zones as being much more active and the interior zones as significantly less active. The attenuation is much greater in the centre of the head since the losses are high in any direction that the photons are taking and, thus, the images without corrected attenuation present lower activity in the centre of the head compared to the cerebral cortex.

The loss of events due to attenuation increases the noise, artifacts and distortion of the image and reduces the reliability of the quantification. Comparatively speaking, the effects of attenuation and scatter are opposite since while attenuation implies a loss of true events, scatter adds false events. Both effects negatively affect correct quantification of the image

Living Brain synthetizes a map of attenuation from the PET image, using segmentation methods to obtain an estimation of brain and cranium volume the attenuation map used is generated in the reconstruction process from an approximated emission image. This image is obtained using 1 OSEM iteration with 12 subsets, in which neither attenuation nor scatter corrections are included. The uncorrected image is radially cropped to remove the noise near the detectors and then segmented using a k-means algorithm with 4 levels. Voxels clustered in the lowest level are considered noise and set to 0, whereas the remaining voxels are set to a uniform value. Afterwards, subsequent mathematical operations are performed in order to fill inner gaps and smooth contours, and finally only the largest connected component is kept.

4. System assembly and validation

4.1 System assembly and validation

All components were individually validated prior to assembly.

Crystals were visually checked for manufacturing defects, and the provider sent a detailed quality control report with the photopeaks of all slabs. All SiPM with similar gains were grouped and assembled together in the same Super-Module, where VBias can be adjusted to a common position.

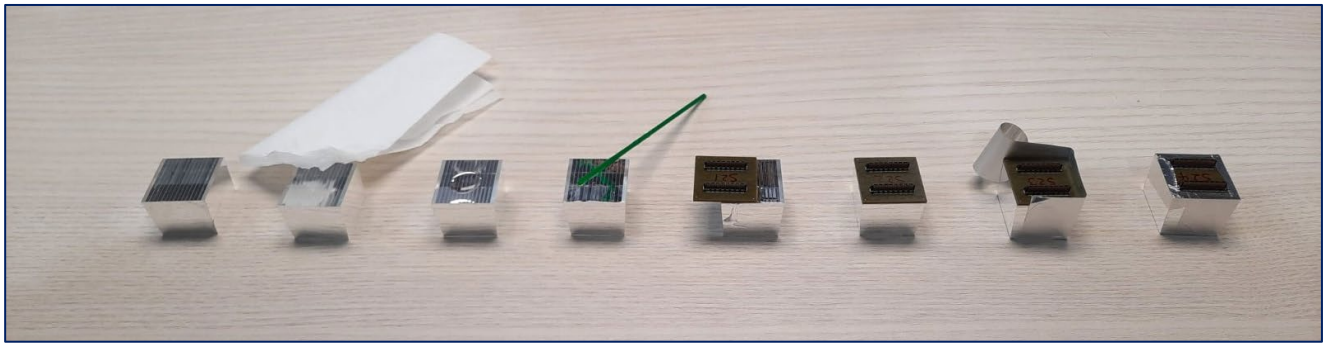

Figure 24: Crystal-SiPM Optical coupling procedure

SiPM were optically coupled with the crystals using a detailed procedure for obtaining similar results for all detector modules (Figure 24). The readout, amplifier and distribution boards were electrically checked for all signals and connected to a calibrated ASIC for flood map verification (Figure 25).

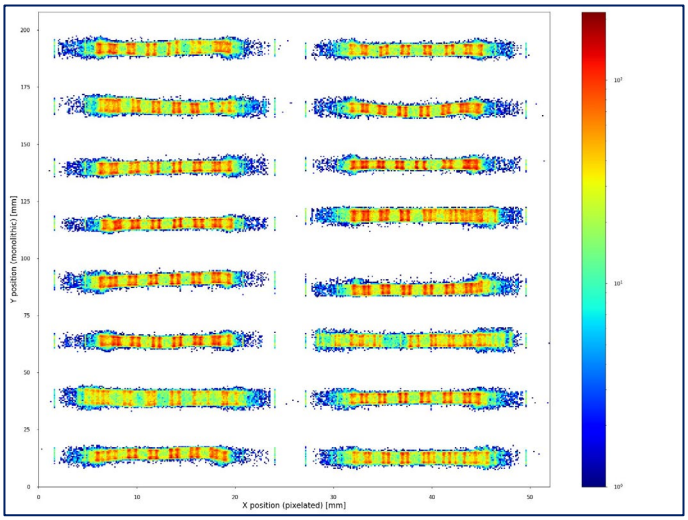

Figure 25: Flood maps

Super-Modules were then assembled and checked electrically before mounting the complete ring.

The cooling system was assembled and checked for leaks before the electronic components of the ring were mounted on the housing. When the complete system was assembled, PETSys electronic was calibrated and all individual channel values verified and, if any error was detected, adjusted.

The flood map of the complete system as well as, the energy spectrums were verified prior to starting the calibration (Figure 26).

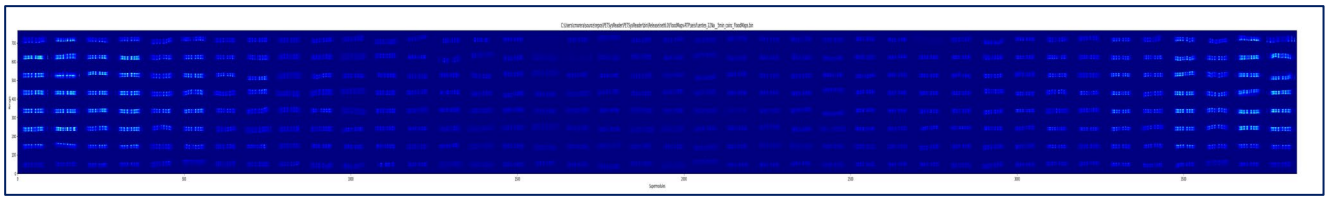

Figure 26: Complete ring flood map

System was installed in May 2023 Hospital La Fe, in Valencia, for final calibration, characterization and patient acquisition (Figure 27).

Figure 27: Instalation at Hospital La Fe

4.2 PET validation

The complete system has been calibrated, and the NEMA protocol has been used for the characterization of the system with good results. The phantoms used to validate the system are a Na-22 point source, an Animal IQ, a Micro-Derenzo phantom and a Hoffman-2D (see: https://search.kg.ebrains.eu/instances/7b135c94-72f7-463a-97e0-4c4821a695c8).

4.2.1 NEMA Validation

Table 1: Living Brain NEMA results

Measurement	Details	Results					
Sensitivity	Na22 Point source, centered in FoV	8.03% max, 30% energy window					
Spatial Resolution	Na22 Point source, centered in FoV	**X axis, FWHM**		**Y axis, FWHM**		**Z axis, FWHM**	
		1.4735 mm		1.3257 mm		2.9194 mm	
Contrast Recovery Coefficient	Animal IQ Phantom, centred	**Rod size**	**1mm**	**2mm**	**3mm**	**4mm**	**5mm**
		Mean	0.08818	0.18371	0.44550	0.66415	0.76796
		Std Dev (%)	16.05194	11.00368	7.46139	6.18498	4.31840
Uniformity	Animal IQ Phantom, centred	**Mean**		**Max**		**Min**	**Std Dev (%)**
		0.01640		0.01928		0.01437	3.75922
Spill-over Ratio	Animal IQ Phantom, centred			**Air**		**Water**	
		Mean		0.26819		0.37006	
		Std Dev (%)		18.34400		11.59657	

4.2.2 Phantom images

Figure 28, Figure 29 and Figure 30 are actual phantom images obtained with the Living Brain system:

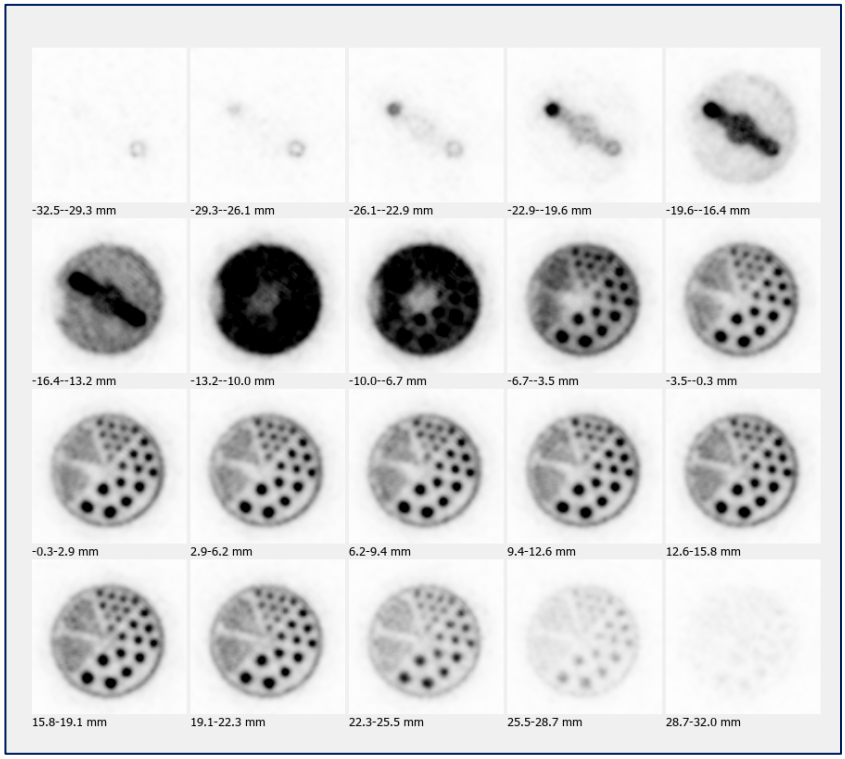

Figure 28: Micro-Derenzo Phantom

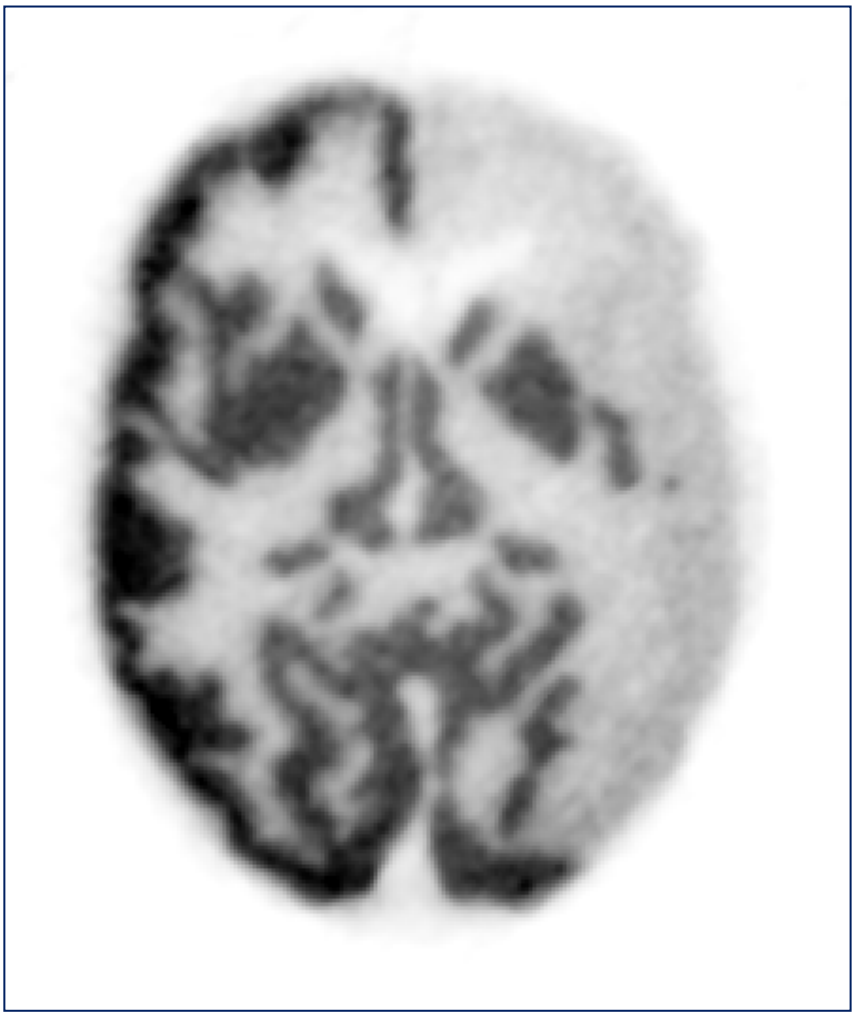

Figure 29: 2D Hoffman (right side only partially filled)

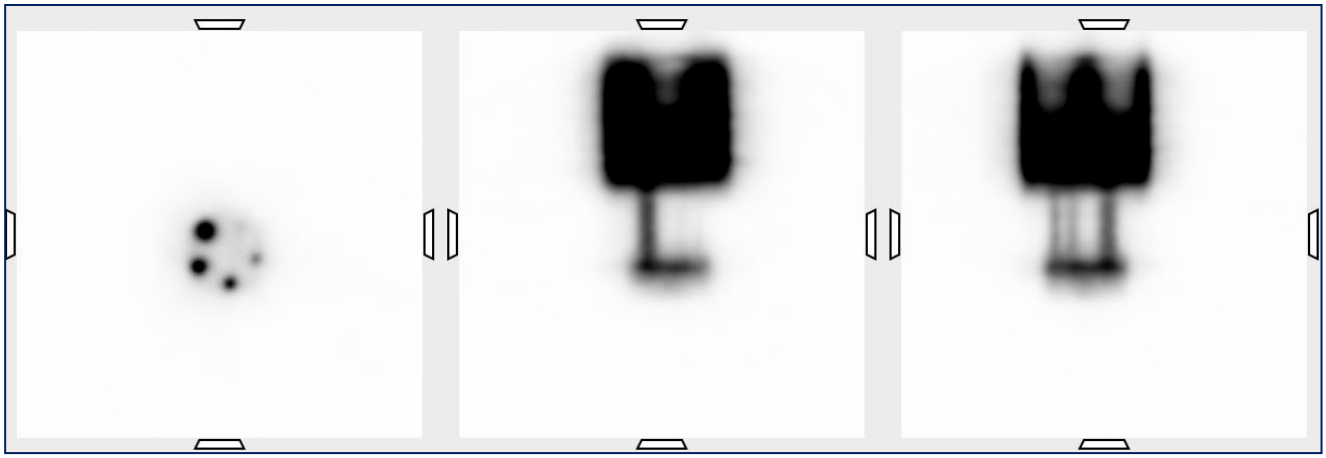

Figure 30: Animal IQ phantom

5. Clinical data acquisition

5.1.1 Clinical trial

A clinical trial for the Proof of Concept in clinical environment has already been approved (see Figure 31) and the first patient was scanned at the end of September. 4 patients are scheduled for end of October. The resulting images will be included in Output OP1.51 (see: https://search.kg.ebrains.eu/instances/9b51cad5-c3a7-4996-a61d-a8aee05729eb).

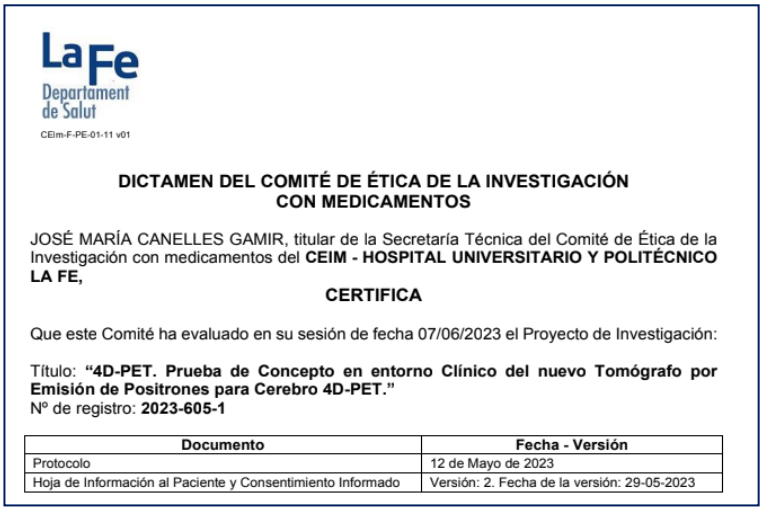

La Fe
Departament de Salut
CEIm-F-PE-01-11 v01

DICTAMEN DEL COMITÉ DE ÉTICA DE LA INVESTIGACIÓN CON MEDICAMENTOS

JOSÉ MARÍA CANELLES GAMIR, titular de la Secretaría Técnica del Comité de Ética de la Investigación con medicamentos del **CEIM - HOSPITAL UNIVERSITARIO Y POLITÉCNICO LA FE,**

CERTIFICA

Que este Comité ha evaluado en su sesión de fecha 07/06/2023 el Proyecto de Investigación:

Título: **"4D-PET. Prueba de Concepto en entorno Clínico del nuevo Tomógrafo por Emisión de Positrones para Cerebro 4D-PET."**
Nº de registro: **2023-605-1**

Documento	Fecha - Versión
Protocolo	12 de Mayo de 2023
Hoja de Información al Paciente y Consentimiento Informado	Versión: 2. Fecha de la versión: 29-05-2023

Figure 31: Ethical committee approval for clinical trial at La Fe, Valencia

6. Looking Forward

An extension of 6 months had to be requested for this deliverable. Currently, the system is already assembled and functional, with excellent preclinical results and outstanding Hoffman phantom images. However, only one patient has been scanned, and the final characterization and assessment are still undergoing, along with all other patients' acquisition to be obtained during October.